

RESEARCH ARTICLE

MicroRNA 155-deficiency leads to decreased autoantibody levels and reduced severity of nephritis and pneumonitis in pristane-induced lupus

Harald Leiss^{1*}, Wilhelm Salzberger¹, Barbara Jacobs¹, Irina Gessl¹, Nicolas Kozakowski², Stephan Blüml¹, Antonia Puchner¹, Attila Kiss³, Bruno K. Podesser³, Josef S. Smolen¹, Georg H. Stummvoll¹

1 Department of Rheumatology, Medical University of Vienna, Vienna, Austria, **2** Department of Pathology Medical University of Vienna, Vienna, Austria, **3** Center for Biomedical Research, Medical University of Vienna, Vienna, Austria

* harald.leiss@meduniwien.ac.at



OPEN ACCESS

Citation: Leiss H, Salzberger W, Jacobs B, Gessl I, Kozakowski N, Blüml S, et al. (2017) MicroRNA 155-deficiency leads to decreased autoantibody levels and reduced severity of nephritis and pneumonitis in pristane-induced lupus. PLoS ONE 12(7): e0181015. <https://doi.org/10.1371/journal.pone.0181015>

Editor: Masataka Kuwana, Keio University, JAPAN

Received: April 5, 2017

Accepted: June 23, 2017

Published: July 18, 2017

Copyright: © 2017 Leiss et al. This is an open access article distributed under the terms of the [Creative Commons Attribution License](https://creativecommons.org/licenses/by/4.0/), which permits unrestricted use, distribution, and reproduction in any medium, provided the original author and source are credited.

Data Availability Statement: All relevant data are within the paper.

Funding: This research has received support from the Innovative Medicines Initiative Joint Undertaking under grant agreement n°115142 (BTCure), resources of which are composed of financial contribution from the European Union's Seventh Framework Programme and EFPIA companies' in kind contribution. The funder had no role in study design, data collection and analysis,

Abstract

Objective

We herein examine the role of endogenous miR155 in the development of systemic manifestations in pristane induced lupus.

Materials and methods

Systemic lupus in miR155-deficient and wild type mice was induced upon injection of pristane and analyzed after 8 months, PBS-injected mice served as controls. Glomerulonephritis and pneumonitis were quantified using the kidney biopsy score and a newly adapted histomorphometric image analysis system; lung tissue was further analyzed by tissue cytometry. Serum levels of anti-dsDNA, anti-histone and anti-chromatin antibodies were measured by ELISA. Frequencies of B cells, activated and regulatory CD4⁺ T cells as well as Th1, Th2, Th17 cells were measured by flow cytometry. RT-qPCR was used to measure expression levels of interferon-signature and T-cell subset related as well as miR155-associated genes.

Results

After induction of lupus, miR155-deficient mice had significant less pulmonary involvement (perivascular inflammatory area in mm²/mm² lung area 0.00092±0.00015 vs. 0.0027±0.00075, p = 0.0347) and renal disease (glomerular activity score 1.95±0.19 vs 3±0.26, p = 0.0029) compared to wild types. MiR155-deficient mice had significantly lower serum levels of disease-associated auto-antibodies and decreased frequencies of activated CD4⁺CD25⁺ (Foxp3⁻) cells. Upon restimulation, CD4⁺ cells showed a less pronounced Th2 and Th17 and a slightly decreased Th1 response in mir155-deficient mice. Pristane-treated wild types showed significantly up-regulated expression of genes related to the INF-signature (MX1, IP10, IRF7, ISG15).

decision to publish, or preparation of the manuscript.

Competing interests: The authors have declared that no competing interests exist.

Conclusions

MiR155-deficient mice had less severe organ involvement, lower serum auto-antibody levels, a less prominent T cell response and lower expressions of genes jointly responsible for disease development. Thus, antagonizing miR155 might be a future approach in treating SLE.

Introduction

Systemic lupus erythematosus (SLE) is a complex autoimmune disorder with abnormal activity of both the adaptive and innate immune systems. Its clinical presentations range from mild musculoskeletal discomfort to life-threatening multiple organ involvement [1, 2].

Pathogenic autoantibodies (abs) are a hallmark of SLE and include those against double-stranded DNA (anti-dsDNA) and other nuclear antigens [3]. Anti-dsDNA serum levels reflect disease activity and are associated with glomerulonephritis [4]. Auto-reactive CD4⁺ T_{effector} cells (or T helper cells, Th) are key players in the pathogenic auto-inflammatory process of the disease [5], since they are expanded, infiltrate affected organs and provide help for B cell activation [6, 7]. On the other hand, regulatory T cells (T_{reg}) are reduced in number and function in active SLE, a potential cause of the loss of peripheral tolerance [8]. Interestingly, T_{reg}-deficient mice exhibit many SLE-like symptoms [9].

Both patients with and experimental animal models of SLE are characterized by an upregulated interferon (IFN) response; type I IFN is a key mediator of innate immunity and appears to play a prominent role in disease pathogenesis [10, 11]. Characteristic type I interferon (IFN-I)-inducible genes like Interferon regulatory factor 7 (IRF7), Interferon gamma-induced protein 10 (IP-10), Interferon-stimulated gene 15 (ISG-15) and MX Dynamin-Like GTPase 1 (Mx1) have been shown to be upregulated in murine and human SLE [11–13] and appear to be related to production of anti-nuclear abs that induce immunopathological damage of various organs [10, 14].

Several mouse models are available to investigate different pathways and mechanisms of the innate and adaptive elements of the immune response in SLE. They usually depend on genetic abnormalities and occur spontaneously [15]. In contrast, pristane induced lupus (PIL) is an inducible type of systemic lupus in otherwise healthy animals without genetic alterations in cells or structures of the immune system [16, 17]. Pristane, a mineral oil (2,6,10,14-tetramethylpentadecane, or TMPD), is known to cause lupus-like disease in humans and induces lupus like disease with characteristic organ involvement and abs in various mouse strains [18–20].

Non-coding RNAs, such as microRNAs (miRs), have been a central point of investigation over the last decade. These small, usually 21–24 nucleotides long RNA molecules modulate gene expression by mediating RNA cleavage, repressing mRNA translation, or causing mRNA destabilization [21]. One of them, miR155, located on chromosome 21, interferes with several aspects of the immune system (B cell-, T cell- and dendritic cell function) and has distinct expression patterns in several diseases [22, 23].

In murine models of systemic autoimmune diseases including SLE, miR155 is overexpressed in T- and B-lymphocytes (spleen) and has been suggested to be a co-trigger of the breakdown of immune tolerance and altered T- and B-cell function [16, 23]. MiR155 promotes the development of inflammatory T cells, including Th17 and Th1 cell subsets, which are known drivers of tissue inflammation [24, 25]. MiR155-deficient mice also have reduced T_{reg}

numbers, both in the thymus and periphery, due to impaired development [26]. Recently, mir155 deficiency was associated with reduced splenomegaly, lower serum IgG antibodies and decreased IgG deposits in glomerula of Fas^{lpr} mice as well as with decreased alveolar hemorrhage in early and aggressive murine lupus [27–29].

Hence, we used an inducible animal model with genetically unaffected immune cells in order to investigate the potential role of miR155 in full-blown SLE eight months after induction. We analyzed thoroughly the extent of inflammatory kidney and lung involvement, tried to gain new insights on T_{effector} and T_{reg} lymphocyte responses as well as on serum auto-antibody levels, and finally analyzed the expression of genes related to the INF-signature which is thought to be a crucial pathway in SLE pathogenesis [10, 11].

Materials and methods

Mice and induction of PIL

Breeding pairs of C57/BL6 (WT) and miR155^{-/-} mice were obtained from The Jackson Laboratory. Generated female WT and miR155^{-/-} littermates were used for this study. At the age of 8–10 weeks (two independent experiments), the mice were injected intraperitoneally (i.p.) with either 0.5 ml of pristane or saline; to facilitate reading C57/BL6 miR155^{-/-} lupus mice will be designated here as PIL^{-/-} (n = 20), and C57/BL6 miR155^{+/+} lupus mice as PIL^{+/+} (n = 20); saline control animals will be accordingly designated as CO^{+/+} (n = 10) and CO^{-/-} (n = 10). Health and behavior of mice were daily assessed. Animals were sacrificed by inhalant anesthetic overdose (ether) followed by cervical dislocation at eight months of age [30]. Animal work was performed under the animal protocol 1919/115-97/98, approved by the animal care committee (Austrian Ministry of Science and Research).

Since in all conducted analysis no clinical or serological differences could be observed between mir155-deficient or wild type control groups, we assumed that miR155 deficiency alone does not lead to lupus like disease [31]. Thus we further compared the pristane groups with the wild type controls (CO^{+/+}) and only with CO^{-/-} if necessary to enhance the clarity of the data.

Clinical assessment, histology and scoring of kidneys

Animals were monitored for clinical signs of glomerulonephritis (GN) by using urine test strips. Post mortem, kidneys, lungs and spleen were obtained from every mouse, prepared and analyzed by histopathologic techniques. Staining with hematoxylin and eosin (HE) allowed a general assessment of inflammation and structural damage, Periodic acid-Schiff (PAS) and acid fuchsin–orange G (SFOG) were used to evaluate glomeruli, blood vessels and immune deposits, respectively. In order to analyze and compare kidney disease severity among the different groups, a blinded pathologist appraised histological features of GN using the composite kidney biopsy score (KBS) and the International Society of Nephrology/Renal Pathology Society (ISN/RPS) classification of lupus nephritis (2003), as described previously [32, 33].

Histological assessment and scoring of lungs

To quantify the detailed histological features of pneumonitis, we assessed histomorphometrical parameters using OsteoMeasure (OsteoMetrics, Decatur, GA, USA), an analysis software which allows to calculate different areas within a histological specimen [34, 35]. We determined areas of (i) perivascular inflammation, (ii) peribronchial inflammation, (iii) the number of perivascular infiltrates and (iv) the number of peribronchial infiltrates as markers of the extent of the pulmonary involvement of SLE and tissue damage in PIL. This method allows a

precise assessment of small (inflammatory) areas in relation to the total area of lung tissue analyzed (mm^2/mm^2) and the possibility to count and mark affected vessels in the OsteoMeasure grid, whereby the number of affected vessels per mm^2 area of lung tissue may be analyzed. When comparing this new OsteoMeasure method with an older (not computer-assisted) method of grading inflammatory pulmonary disease, we found a high correlation of the results (perivascular inflammatory area: Pearson $r = 0.76$, $p = 0.001$; total inflammatory area: Pearson $r = 0.84$, $p < 0.0001$) [36].

Additional immunohistochemistry using abs against macrophages (clone F4/80, AbD Serotec, Oxford, UK), granulocytes (Neu7/4, AbD Serotec), T- (anti-CD3, Novo Castra Laboratories, Newcastle, UK) and B-cells (anti-CD45 receptor, BD Biosciences PharMingen, San Diego, CA, USA) [37] and quantitative analysis of the inflammatory cellular infiltrate was performed by tissue cytometry using cell-identification algorithms for nuclear segmentation (HistoQuest, TissueGnostics, Vienna, Austria) in order to assess the composition of these infiltrates [38, 39].

Detection of auto-antibodies

Anti-dsDNA auto-antibodies were measured by enzyme-linked immunosorbent assay (ELISA) using mouse monoclonal anti-dsDNA IgG (Alpha Diagnostic International, San Antonio, TX) as standard and horseradish conjugated goat-anti-mouse IgG antibody (Dianova, Hamburg, GER) as described previously [40]. Sera were added at a 1:1000 dilution in 1% BSA/PBS for 1h at room temperature. Results are displayed in absorbance units. Anti-histone and anti-chromatin antibodies (abs) were measured by ELISA (Inova Diagnostics, San Diego, USA) as described before [30]. Results are presented as units/ml (U/ml) employing the reference sera provided by the manufacturer.

Flow cytometry

Lymphocytes were isolated from spleens after organ removal and analyzed separately for each mouse by flow cytometry. Cell surface stainings were performed according to standard procedures using antibodies against CD4, CD8, CD19 and CD25 directly conjugated to fluorescein isothiocyanate (FITC) or phycoerythrin (PE) purchased from BD Pharmingen (San Diego, CA). Anti-CD4-Tri-Color was purchased from Caltag Laboratories (Hamburg, GER). Monoclonal antibodies (mAbs) for intracellular stainings (anti-IL-4⁺, anti-IL-17⁺, anti-IFN γ ⁺) conjugated to PE or allophycocyanin (APC) were purchased from BD Pharmingen. PE- or FITC-labelled mAbs to FoxP3 were from eBioscience (Vienna, AUT). Intracellular cytokine staining was performed with PE- or APC- labelled mAbs as described [41]. In brief, isolated cells were stimulated with plate-bound anti-mouse CD3e mAbs (clone 145-2C11), and anti-mouse CD28 mAbs (clone 37.51, both BD Pharmingen) at $1\mu\text{g}/\text{ml}$ for 5 hours under the presence of BD-GolgiStop Protein Transport Inhibitor (containing Monensin, BD Biosciences, San Diego, CA). All flow cytometry was performed on a FACSCanto II and analyzed using FACSDiva software (all from BD Biosciences). The main cell types were quantified as their percentage in the entire lymphocyte populations, while T-cell subsets were quantified as their percentage in CD4⁺ lymphocyte populations.

Messenger RNA(mRNA) quantitative RT-qPCR

Total RNA was isolated from spleens using RNeasy mini kit (Qiagen, Hilden, GER). cDNA was prepared using Omniscript RT kit (Qiagen), followed by SYBR Green-based RT-qPCR (Roche Molecular Biochemicals/ Sigma-Aldrich, Vienna, AUT)) using the Light cycler 480 (Roche Molecular Biochemicals). Following primers were used: MX1:

5' -GATCCGACTTCACTTCCAGATGG- '3 and 5' -CATCT-CAGTG-GTAGTCAACCC-'3 ; IP-10: 5' -ATCATCCCTGCGAGCCTAT- '3 and 5' -ATTCTTGCTTCGGCAGTTAC- '3 ; IRF7: 5' -GAGCTTGGATCTACTGTGG- '3 and 5' -TAGAAAGCAGAGGGCTTG- '3 ; ISG15: 5' -CAGAAGCAGACTCCTTAATTC- '3 and 5' -AGACCTCATAGATGTTGCTGTG- '3 ; IFIT1: 5' -TCTACGCGATGTTTCCTACG- '3 and 5' -TGTGAAGCAGAAGCACACA- '3 ; IFIT3: 5' -ACTTGCATGAGCATGGCTTT- '3 and 5' -AGCACTCAGGAGTGGAGTGG- '3 ; STAT1: 5' -CTGAATATTTCCCTCCTGGG- '3 and 5' -TCCCGTACAGATGCCATGAT- '3 ; FOXO3: 5' -AGTGGATGGTGCCTGTGT- '3 and 5' -CTGTGCAGGGACAGTTGT- '3 ; SOCS1: 5' -ACAAGCTGCTACAACCAGGG- '3 and 5' -ACTTCTGGCTGGAGACCTCA- '3 ; SHIP1: 5' -CCAGGGCAAGATGAGGGAGA- '3 and 5' -GGACCTCGGTTGGCAATGTA- '3 ; INF γ : 5' -AGCGGCTGACTGAACTCAGA-TTGTA- '3 and 5' -GTCACAGTTTTTCAGCTGTATAGG G- '3 ; IL4: 5' -CGAGAACACAC-AGGAGTGAGCT- '3 and 5' -GACTCATTCATGGTGCAGC TTATCG- '3 ; IL17: 5' - TCT-CATCCAGCAAGAGATCC- '3 and 5' -AGTTTGGGACCCCT TTACAC- '3 ; TNFSF13b: 5' -GCCTTCCATCCCTGCAGAT- '3 and 5' -CCATCACTCCGC AGAAGGA- '3 ; IRF1: 5' -AGCAGTTCTTTGGGAATAGG- '3 and 5' -CCCACAGAAGAGCAT AGCAC- '3 ; GAPDH: 5' -TGGCATTGTGGAAGGGCT-CATGAC- '3 and 5' -ATGCCAGTG AGCTTGCCGTTTC-AGC- '3 was used as an internal control. The relative expression of the mRNA of the gene of interest was calculated by the $2^{-\Delta\Delta CT}$ method.

Statistical analysis

All group results are expressed as mean \pm SD, if not stated otherwise. Student's t-test, or Fisher's exact test (2-tailed) were used for the comparison of group values and discriminatory parameters, where appropriate. For comparing group values that did not follow Gaussian distribution, Mann-Whitney's test (2-tailed) was used. Welch's correction was applied if variances were significantly different. Pearson and Spearman correlation coefficients were calculated for variables following, or not-following Gaussian distributions, respectively. P values less than 0.05 were considered significant. All statistical analyses were performed using Prism 6 for Mac OS X (Version 6.0d, October 15, 2013) software.

Results

Reduced lupus-associated auto-abs in miR155^{-/-} mice

In line with previous findings PIL^{+/+} mice developed high levels of anti-dsDNA, anti-chromatin, and anti-histone-abs after induction of PIL [18, 30]. In contrast, anti-dsDNA, anti-chromatin and anti-histone levels were significantly lower in PIL^{-/-} animals and only minimally increased than in CO^{+/+} (Fig 1A–1C). Thus, miR155 deficiency abrogated or at least significantly reduced the autoantibody response in PIL.

Effects of miR155 deficiency on lymphocyte subsets

After disease induction miR155-deficient PIL^{-/-} mice showed lower frequencies of B-cells and CD4⁺ cells compared to wild type lupus group PIL^{+/+}; no difference was seen between the former and controls (Fig 2A and 2B). In contrast, we did not find differences in frequencies of CD8⁺ cells between the groups (Table 1).

Frequencies of activated CD4 T-cells and regulatory T-cells in miR155 deficiency. In PIL^{+/+}, activated CD4⁺CD25⁺Foxp3⁻ T_{effector}-cells were significantly increased compared to controls and compared to less active disease as seen in PIL^{-/-} when assessed by flow cytometry; PIL^{-/-} had slightly, but not significantly higher frequencies than CO^{+/+} (Fig 2C). In addition, PIL^{+/+} had lower numbers of regulatory T cells (T_{reg}, CD4⁺CD25⁺Foxp3⁺ cells) and an

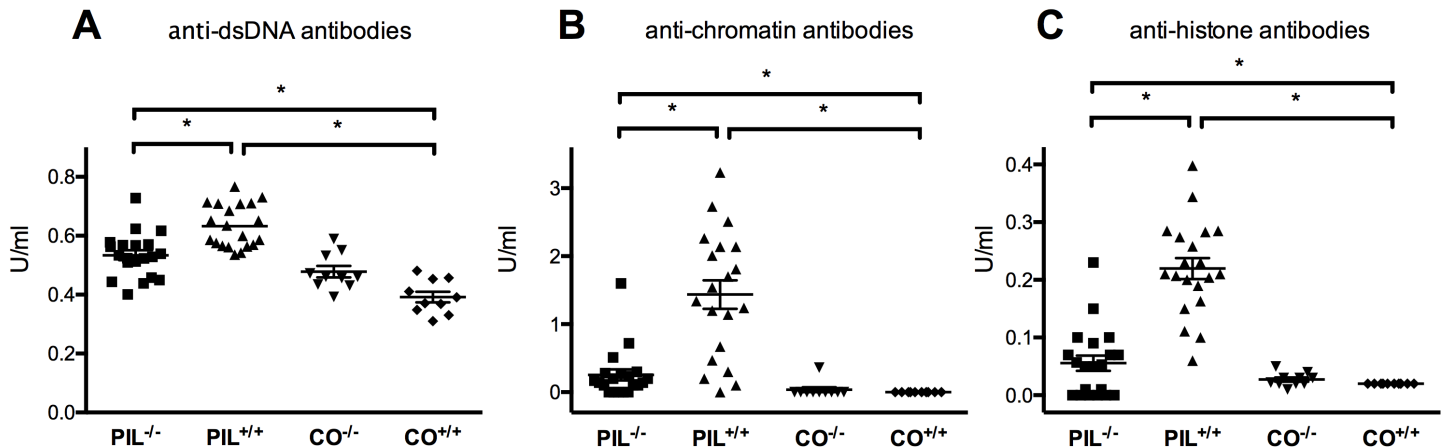


Fig 1. Anti-dsDNA, anti-chromatin and anti-histone auto-antibody levels at 8 months after disease induction. A, Anti-dsDNA IgG antibody levels were significantly lower in mir155-deficient PIL^{-/-} than in lupus wild type PIL^{+/+}. Both pristane-induced groups, PIL^{+/+} and PIL^{-/-}, had significantly increased antibody levels compared to CO^{+/+}. B, C, In addition, PIL^{-/-} also had lower levels of anti-chromatin-antibodies and anti-histone-antibodies than PIL^{+/+}. Antibody levels in PIL^{-/-} were only slightly elevated compared to CO^{+/+}. Results are representative of 2 independent experiments. PIL were induced with pristane, CO with PBS; ^{+/+} stands for wild type, ^{-/-} for miR155-deficient knockouts; bars show mean with SD. * = P < 0.05, by Mann-Whitney test.

<https://doi.org/10.1371/journal.pone.0181015.g001>

increased activated T_{effector}/T_{reg} ratio compared to the respective healthy controls (CO^{+/+}) (Fig 2D). In line with the literature, T_{reg} showed lower yields in both mir155-deficient groups (Table 1 and 1.48±0.15 in CO^{-/-}, respectively) [26]. As in wild typed, the pristane injected knockout group (PIL^{-/-}) had higher frequencies of activated T_{effector} cells and an increased activated T_{effector}/T_{reg} ratio compared to the respective control (CO^{-/-}) (Table 1 and 0.77±0.17 for CO^{-/-}, respectively).

Analysis of CD4⁺ T-cell subsets. Upon *in vitro* stimulation, the frequencies of Th1 cells (CD4⁺IFNγ⁺) in both pristane injected groups (PIL^{+/+} and PIL^{-/-}, respectively) were elevated compared to CO^{+/+} and slightly, albeit not significantly, elevated in PIL^{+/+} compared to PIL^{-/-} (when analyzed by flow cytometry (Fig 2E)). In PIL^{+/+}, both frequencies of Th2 (CD4⁺IL-4⁺) and Th17 (CD4⁺IL17⁺) cells were increased compared to PIL^{-/-} or controls (Fig 2F and 2G, all statistics in Table 1).

In order to confirm these results we also analyzed the expression of IFNγ, IL-4 and IL-17 in splenocytes by RT-qPCR and found significant upregulation in PIL^{+/+} compared to PIL^{-/-} and CO^{+/+} after induction of PIL (Fig 3B).

Decreased severity of kidney involvement in miR155-deficient mice

The summative kidney biopsy score (KBS) of PIL^{+/+} was significantly higher than that of PIL^{-/-}, which did not significantly differ from controls (Fig 4A). In addition, the glomerular activity score (GAS), mainly reflecting glomerular cellular changes, was significantly higher in PIL^{+/+} compared to PIL^{-/-} and CO^{+/+} (Fig 4B). Concerning the chronic lesion score (CLS), there were no differences between the two PIL groups, both being significantly higher than CO^{+/+} (Fig 4C and Table 2).

Applying the ISN/RPS 2003 classification for lupus nephritis, all 20 PIL^{+/+} mice, but only 60% (12/20) of PIL^{-/-} exhibited signs of damage (p = 0.0033). In addition, nephritis was more severe in PIL^{+/+} (40% proliferative GN (resembling human class III focal lupus nephritis), 60% mesangial GN (resembling human class II mesangial proliferative lupus nephritis)), while PIL^{-/-} only had mild mesangial GN (Fig 4G–4I and Table 2).

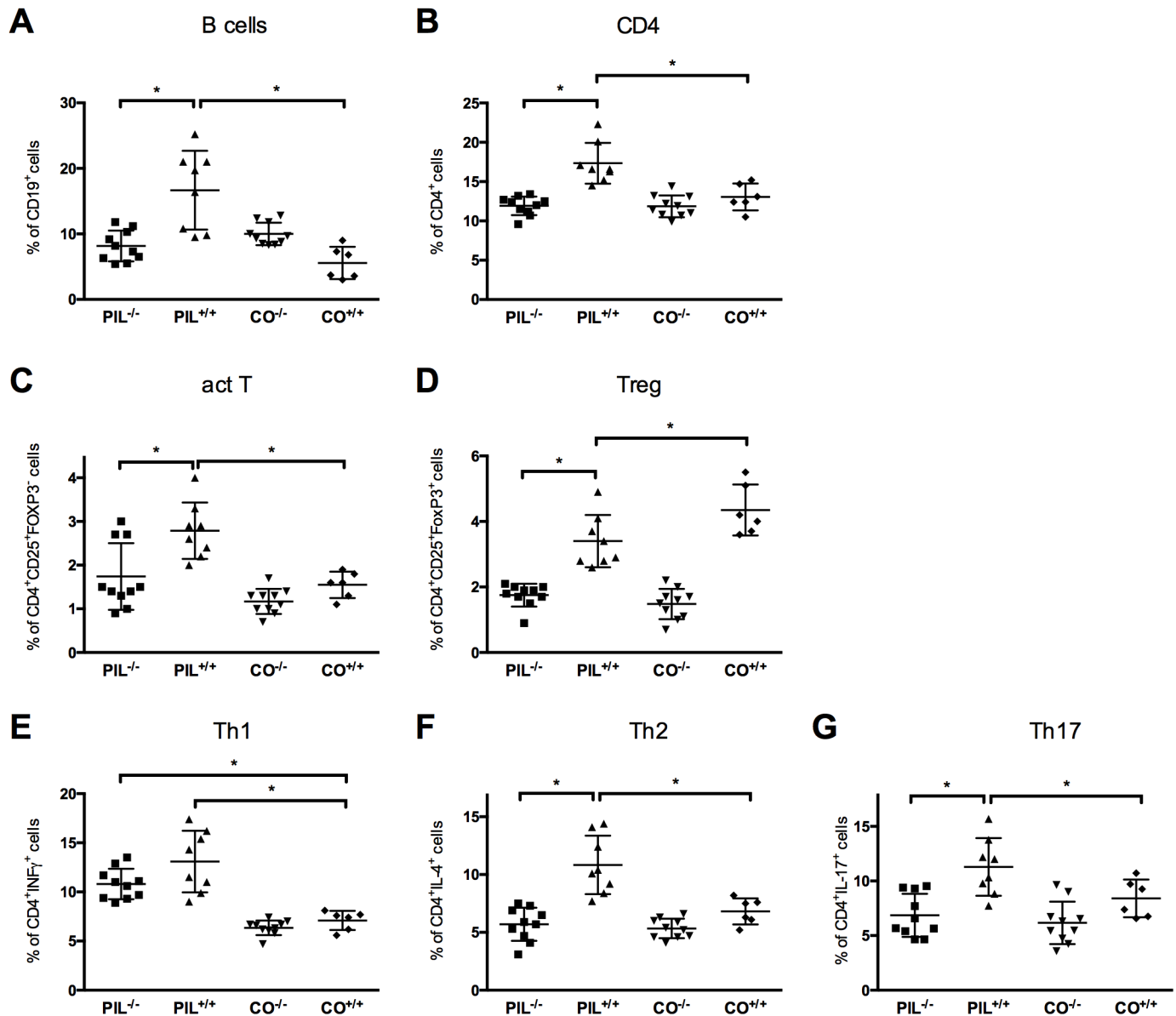


Fig 2. Flow cytometry analysis of lymphocyte subsets at 8 months after disease induction. A, B, C, MiR155-deficient $PIL^{-/-}$ mice had lower frequencies of $CD19^{+}$ B-cells, total $CD4^{+}$ and $CD4^{+}CD25^{+}FoxP3^{-}$ activated $T_{effector}$ -cells compared to the WT lupus group $PIL^{+/+}$. D, Frequencies of $CD4^{+}CD25^{+}Foxp3^{+}$ regulatory T cells (T_{reg}) were reduced in $PIL^{+/+}$ compared to the respective control group ($CO^{+/+}$). T_{reg} were even lower in both miR155 knockout groups ($PIL^{-/-}$ and $CO^{-/-}$) without intergroup differences. E, F, G, Upon *in vitro* restimulation, $PIL^{+/+}$ had significant higher frequencies of $CD4^{+}IL-4^{+}$ Th2 and $CD4^{+}IL-17^{+}$ Th17 cells compared to $PIL^{-/-}$ and $CO^{+/+}$, a similar, albeit not significant trend was observed for $CD4^{+}IFN\gamma$ Th1 cells when comparing $PIL^{+/+}$ to $PIL^{-/-}$. See also Table 1 for exact numbers and p values. Results are representative of 2 independent experiments. PIL were induced with pristane, CO with PBS; $+/+$ stands for wild type, $-/-$ for miR155-deficient knockouts; bars show mean with SD. * = $P < 0.05$, by Mann-Whitney test.

<https://doi.org/10.1371/journal.pone.0181015.g002>

Decreased severity of lung involvement in miR155-deficiency

Pneumonitis with perivascular inflammatory infiltration is a major organ manifestation of SLE [42]. Using image analysis (OsteoMeasure), the perivascular inflammatory area was significantly reduced in $PIL^{-/-}$ compared to $PIL^{+/+}$. (Fig 4D). Both PIL groups also showed peribronchial inflammation with a trend towards more pronounced inflammation in $PIL^{+/+}$ (Fig 4E).

Table 1. Detailed results for lymphocyte subsets in wild type lupus (PIL^{+/+}), miR155-deficient lupus (PIL^{-/-}) and controls (CO^{+/+}) as assessed by flow cytometry.

Cell-frequencies in % (mean±SD)	PIL ^{+/+}	PIL ^{-/-}	CO ^{+/+}	p-value	p-value	p-value
				PIL ^{+/+}	PIL ^{-/-}	PIL ^{+/+}
				vs. PIL ^{-/-}	vs. CO ^{+/+}	vs. CO ^{+/+}
CD19 ⁺	16.67±2.78	8.18±1.58	5.57±1.01	0.0269	ns.	0.0062
CD4 ⁺	17.37±1.06	11.98±0.58	13.05±0.7	0.0017	ns.	0.0066
CD8 ⁺	7.59±0.67	7.81±0.77	9.3±0.9	ns.	ns.	ns.
CD4 ⁺ CD25 ⁺ Foxp3 ⁻	2.79±0.23	1.74±0.24	1.55±0.12	0.0061	ns.	0.0007
CD4 ⁺ CD25 ⁺ Foxp3 ⁺	3.40±0.28	1.76±0.12	4.35±0.32	0.0004	0.0002	0.0465
Activated T _{effector} /T _{reg} ratio	0.86±0.1	0.99±0.17	0.36±0.03	ns.	0.0068	0.0014
CD4 ⁺ INF γ ⁺	13.09±1.25	10.83±0.86	7.1±0.4	ns.	0.0151	0.0024
CD4 ⁺ IL-4 ⁺	10.83±1.47	5.7±1.09	6.83±0.67	0.0229	ns.	0.0426
CD4 ⁺ IL17 ⁺	11.29±0.93	6.86±0.79	8.4±0.7	0.0028	ns.	0.0296

<https://doi.org/10.1371/journal.pone.0181015.t001>

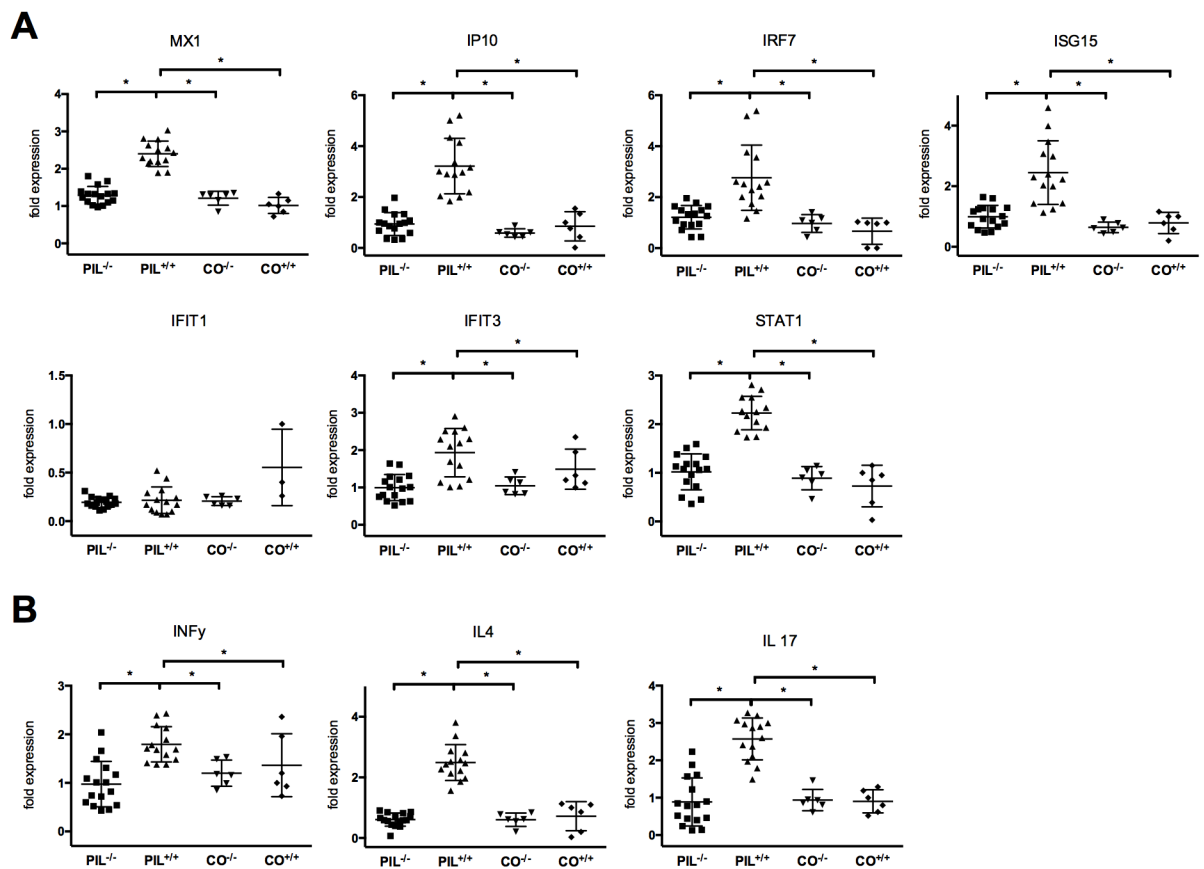


Fig 3. Analysis of gene-expression patterns of INF-signature related genes and T-cell subset related cytokines. A, After induction of PIL in contrast to the mir155-deficient group PIL^{-/-} and controls (CO^{+/+}), INF-related genes were upregulated in the lupus wild type group PIL^{+/+}. B, Cytokines related to the T-cell subsets (Th1, Th2, Th17) were significantly upregulated in PIL^{+/+}, but not in PIL^{-/-} and CO^{+/+}. Results are representative of 2 independent experiments. PIL were induced with pristane, CO with PBS; ^{+/+} stands for wild type, ^{-/-} for miR155-deficient knockouts; bars show mean with SD. * = *P* < 0.05, by Mann-Whitney test.

<https://doi.org/10.1371/journal.pone.0181015.g003>

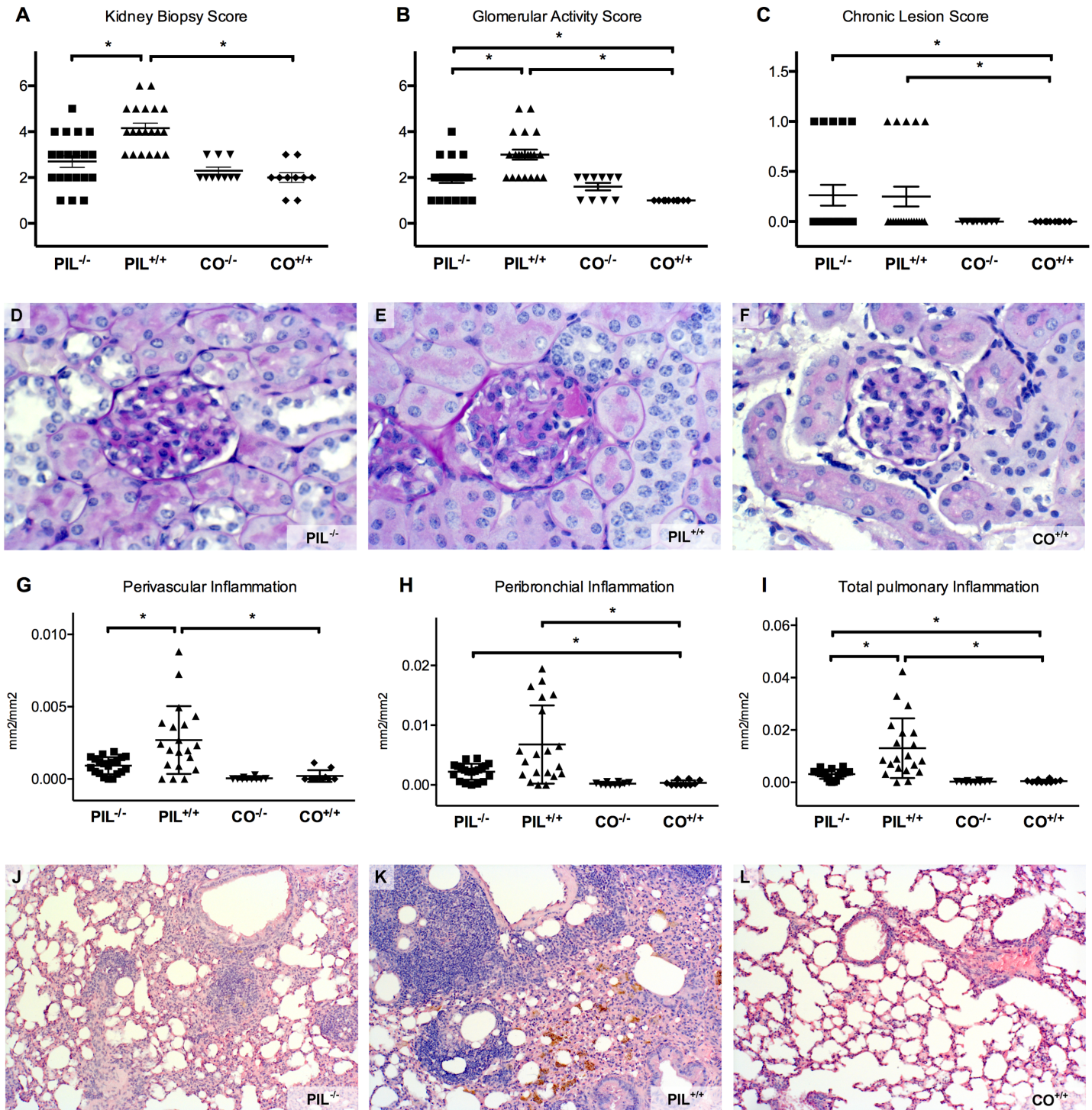


Fig 4. Renal and pulmonary involvement in fully established pristane-induced lupus (PIL). A, B, C, The summative kidney biopsy score and the glomerular activity score of wildtype lupus PIL^{+/+} was significantly higher than that of mir155-deficient PIL^{-/-}, while there was no difference in the chronic lesion score. D, E, F, If affected, PIL^{-/-} showed only mild mesangial glomerulonephritis. PIL^{+/+} had more severe renal manifestation with increased cellularity and hyaline deposits (black arrow). 40% of PIL^{+/+}, but no PIL^{-/-}, fulfilled the criteria for proliferative glomerulonephritis, while controls were not affected. G, H, I, Although all PIL mice showed at least some pulmonary pathology, the inflammatory perivascular area as well as the area of peribronchial and total pulmonary inflammation were greater in PIL^{+/+} than in PIL^{-/-}, while controls were not affected. J, K, L, Typical examples show the marked pulmonary inflammation in PIL^{+/+} compared to PIL^{-/-} or controls; PIL^{+/+} also had considerable hemosiderin deposits as a late consequence of intrapulmonary bleeding (white arrow). Results are representative of 2 independent experiments upon analysis at 8 months after disease induction. PIL were injected with pristane, CO with PBS; +/- stands for wild type, -/- for miR155-deficient knockouts; bars show mean with SD, * = p< 0.05.

<https://doi.org/10.1371/journal.pone.0181015.g004>

Table 2. In-depth analysis of the organ involvement of miR155-deficient PIL^{-/-} compared to wild type lupus PIL^{+/+} and wild type controls CO^{+/+}.

	PIL ^{+/+}	PIL ^{-/-}	CO ^{+/+}	p-value PIL ^{+/+} vs. PIL ^{-/-}	p-value PIL ^{-/-} vs. CO ^{+/+}
Kidney (mean±SD)					
Glomerular activity Score	3±0.26	1.95±0.19	1±0	0.0029	0.0001
Tubulointerstitial activity Score	0.88±0.24	0.47±0.14	1±0.26	ns.	ns.
Chronic lesion Score	0.26±0.10	0.25±0.11	0±0	ns.	0.0207
Kidney Biopsy Score	4.13±0.27	2.68±0.27	2±0.26	0.0006	0.0831
ISN/RPS classification	40% III/ 60% II	100% II	10% II	-	-
Lungs (mean±SD)					
OsteoMeasure					
Perivascular	0.0027±	0.00092±	0.0002±	0.0347	ns.
Inflammation (mm²/mm²)	0.00075	0.00015	0.0001		
Number of perivascular changes (#/mm²)	0.81±0.19	0.48±0.09	0.02±0.02	ns.	<0.0001
Peribronchial	0.0068±	0.00225±	0.0003±	ns.	0.0001
Inflammation (mm²/mm²)	0.0025	0.0003	0.0002		
Total pulmonary	0.0013±	0.0031±	0.0005±	0.01	0.0034
Inflammation (mm²/mm²)	0.0033	0.0004	0.0002		
Immunohistochemical Stainings					
Perivascular areas					
T cells (#/mm²)	3911.2	232.6	-	<0.0001	-
B cells (#/mm²)	4721.1	2611.9	-	<0.0001	-
Neutrophil Granulocytes (#/mm²)	3208.9	757.7	-	<0.0001	-
Macrophages (#/mm²)	575.1	247.1	-	<0.0001	-
Peribronchial areas					
T cells (#/mm²)	834.1	595.8	-	ns.	-
B cells (#/mm²)	1414.7	226.2	-	<0.0001	-
Neutrophil Granulocytes (#/mm²)	1112.8	1107.8	-	ns.	-
Macrophages (#/mm²)	2513.4	1798.5	-	ns.	-

<https://doi.org/10.1371/journal.pone.0181015.t002>

In summary, total inflammation was significantly higher in PIL^{+/+} than in respective PIL^{-/-} group (Fig 4F and 4J–4L).

In line with the quantitative analysis of the histological lung involvement, the immunohistochemical stainings of affected perivascular areas in PIL^{-/-} showed less accumulation of CD3 positive T cells (Fig 5A and 5E), CD45R positive B cells (Fig 5B and 5F), F4/80 positive macrophages (Fig 5C and 5G) and Neu7/4 positive neutrophil granulocytes (Fig 5D and 5H) compared to PIL^{+/+}. In peribronchial infiltrates, the composition of cells did not differ significantly between the two lupus groups, except for a reduced number of B cells in mir155-deficient mice (all statistics shown in Table 2).

The impact of miR155 deficiency on the expression patterns of the INF-signature and T-cell subset related cytokines

We next determined INF-signature genes in splenic cells using RT-qPCR in PIL. We detected significant upregulation of IFN-related genes in PIL^{+/+} compared to CO^{+/+}, consistent with an IFN signature after induction of PIL. In contrast, no upregulation of this set of genes was

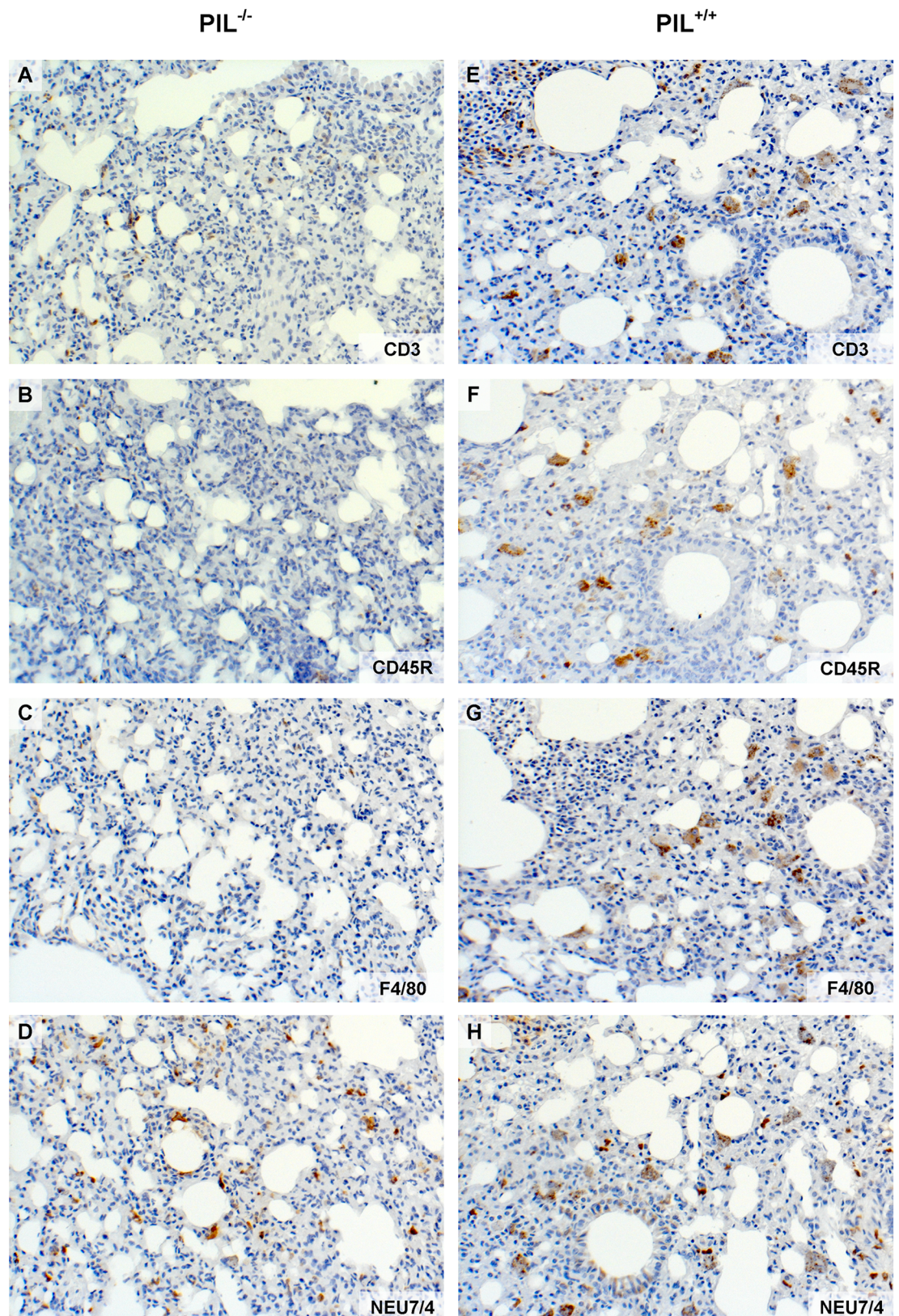


Fig 5. Immunohistochemical stainings of affected lungs. A, E, The miR155-deficient group $PIL^{-/-}$ showed less accumulation of CD3 positive T cells that the lupus wild type group $PIL^{+/+}$. The same effect was observed in other

immunohistochemical stainings: B, F, CD45R positive B cells, C, G, F4/80 positive macrophages and D, H, Neu7/4 positive neutrophil granulocytes. See also Table 1 for exact numbers and p values. Results are representative of 2 independent experiments. PIL were induced with pristane; ^{+/+} stands for wild type, ^{-/-} for miR155-deficient knockouts.

<https://doi.org/10.1371/journal.pone.0181015.g005>

detectable after induction of PIL in miR155 deficient mice (PIL^{-/-}) (Fig 3A). In addition, analysis of cytokines related to the T-cells subsets (Th1, Th2, Th17) were also significantly upregulated in PIL^{+/+} compared to PIL^{-/-} and CO^{+/+} after induction of PIL (Fig 3B).

Discussion

Given that the etiology of SLE has not been fully elucidated, current therapies, although effective in many cases, still show major limitations. MiR155, as a molecule potentially involved in lupus pathogenesis, might constitute an interesting therapeutic target [28].

Compared to wild type mice, we found reduced disease severity with respect to pulmonary and renal manifestations in mir155-deficient mice after induction of systemic lupus. In addition, also B cell counts and levels of SLE-typical auto-antibodies, such as anti-dsDNA, anti-histone and anti-chromatin abs, were decreased in mir155-deficient mice, albeit still slightly elevated compared to controls (Figs 1, 2, 3 and 4).

Since miR155 is known to promote autoimmune inflammation by enhancing inflammatory T cells, we analyzed T cell subsets in mir155-deficient lupus [26]. In line with observations in mir155-deficient non-lupus animals, we observed a reduction of activated T_{effector} cells with lower Th17 frequencies and a trend toward lower IFN γ -producing Th1 cells in mir155-deficient PIL^{-/-} mice compared to PIL^{+/+} animals [24, 43, 44]. Interestingly, and in contrast to the reported tendency of miR155^{-/-} lymphocytes to produce IL-4 rather than IFN γ , we also found a significantly lower frequency of IL-4 producing Th2 cells in pristane-induced miR155^{-/-} mice than in wild type PIL [22]. These results gained by flow cytometry upon *in vitro* restimulation could be confirmed by RT-qPCR for the respective cytokines (Figs 2 and 5).

Since elevated counts of activated T_{effector} cells as well as reduced numbers and functional properties of T_{reg} are a known feature of active SLE, it was not surprising that we found (in accordance with disease severity) increased frequencies of CD4⁺CD25⁺ T_{effector} cells and an increased ratio of T_{effector}/T_{reg} cells in PIL^{+/+} mice compared to less active PIL^{-/-} knockout mice or controls [1, 8]. Interestingly (and in line with the literature), miR155-deficient animals had reduced numbers of CD4⁺FoxP3⁺T_{reg} cells irrespective of the induction of systemic autoimmunity by the pristane trigger, which is due to an impaired thymic development [26, 45]. Given the fact that a complete lack of functional CD4⁺FoxP3⁺ cells leads to severe autoimmune disease with a variety of lupus-like symptoms, these T_{reg} in miR155^{-/-} mice are likely still functional, since peripheral tolerance is still maintained in mir155-deficient controls (CO^{-/-}) which did not show any signs of inflammation or autoimmune disease [9].

As a main factor of SLE pathogenesis, an upregulation of type I IFN is postulated (“IFN-signature”) and has also been reported in PIL [10, 11]. Since miR-155 has been shown to regulate type I IFN responses by targeting IFN signaling components, we hypothesized that the reduction in lupus manifestations could be due to effects in the IFN pathway and found a reduced expression of various IFN related genes (MX1, IP10, IRF7, ISG15, IFIT3, STAT1) in PIL^{-/-} when compared to wild type PIL^{+/+} [46].

MiR155 is attributed with a role in the pathogenesis of many autoimmune disorders like SLE or rheumatoid arthritis, but the complex orchestra of its effects on pro- and anti-inflammatory pathways is still under investigation and not fully elucidated yet [23]. A recent publication could show that miR155 gene expression in lung tissue increased within 7 days after pristane injection as did genes encoding for toll-like receptor 4 (TLR-4), TLR-7 and TLR-2

and mitogen-activated protein kinase (MAPK) pathways that encode pro-inflammatory cytokines (e.g. TNF receptor factor 6 [TRAF6]) and genes related to the IL-6 and TNF signaling pathways [28]. In mir155-deficient mice, however, there was a reduced activation of the MAPK and TLR pathways upon stimulation with pristane and decreased levels of IL-6 and TNF [27, 28, 38]. In addition to its effects on the MAPK pathway, miR155 also targets multiple inflammatory pathways like the c-Jun N-terminal kinase (JNK) [47], and, as we could show herein, also genes related to the IFN type I activation which is considered crucial in SLE pathogenesis [10, 11].

In summary, we could demonstrate that mir155-deficient mice develop less severe manifestations of systemic lupus than seen in genetically normal C57/BL6 mice: *PIL^{-/-}* mice show less severe renal and pulmonary involvement, lower levels of anti-dsDNA, -chromatin and -histone abs, have reduced frequencies of activated T- cell and B-cell populations and a less pronounced INF signature.

Conclusions

Since despite all efforts still many SLE patients do not sufficiently respond to current concepts of therapy and since the application of a miR155 antagomir could reduce early diffuse alveolar hemorrhage (DAH) in experimental lupus, miR155 might become an interesting aspect in treating (refractory) lupus [28]. A further understanding of the role of miRNAs, and miR155 in particular, might allow for the identification of a new therapeutic strategy in SLE.

Acknowledgments

The authors acknowledge B. Niederreiter, T. Shvets, C.W. Steiner.

Author Contributions

Conceptualization: Harald Leiss, Stephan Blüml, Josef S. Smolen, Georg H. Stummvoll.

Data curation: Harald Leiss, Wilhelm Salzberger, Barbara Jacobs, Irina Gessl.

Formal analysis: Harald Leiss, Wilhelm Salzberger, Barbara Jacobs, Irina Gessl, Antonia Puchner.

Funding acquisition: Josef S. Smolen.

Investigation: Harald Leiss, Wilhelm Salzberger, Barbara Jacobs, Irina Gessl, Nicolas Kozakowski, Antonia Puchner.

Methodology: Harald Leiss, Stephan Blüml, Georg H. Stummvoll.

Project administration: Harald Leiss, Georg H. Stummvoll.

Resources: Attila Kiss, Bruno K. Podesser, Josef S. Smolen.

Supervision: Josef S. Smolen, Georg H. Stummvoll.

Validation: Josef S. Smolen, Georg H. Stummvoll.

Visualization: Harald Leiss.

Writing – original draft: Harald Leiss, Georg H. Stummvoll.

Writing – review & editing: Harald Leiss, Wilhelm Salzberger, Barbara Jacobs, Irina Gessl, Nicolas Kozakowski, Stephan Blüml, Antonia Puchner, Attila Kiss, Bruno K. Podesser, Josef S. Smolen, Georg H. Stummvoll.

References

1. Scheinecker C, Bonelli M, Smolen JS. Pathogenetic aspects of systemic lupus erythematosus with an emphasis on regulatory T cells. *Journal of autoimmunity*. 2010; 35(3):269–75. Epub 2010/07/20. <https://doi.org/10.1016/j.jaut.2010.06.018> PMID: 20638240.
2. Stummvoll G, Stamm T. The patients' perspective: Living with Lupus in Austria. *Wien Klin Wochenschr*. 2017;in press.
3. Rahman A, Isenberg DA. Systemic lupus erythematosus. *N Engl J Med*. 2008; 358(9):929–39. Epub 2008/02/29. <https://doi.org/10.1056/NEJMra071297> PMID: 18305268.
4. ter Borg EJ, Horst G, Hummel EJ, Limburg PC, Kallenberg CG. Measurement of increases in anti-double-stranded DNA antibody levels as a predictor of disease exacerbation in systemic lupus erythematosus. A long-term, prospective study. *Arthritis Rheum*. 1990; 33(5):634–43. Epub 1990/05/01. PMID: 2346519.
5. Choi J, Kim ST, Craft J. The pathogenesis of systemic lupus erythematosus—an update. *Curr Opin Immunol*. 2012; 24(6):651–7. Epub 2012/11/08. PubMed Central PMCID: PMC3508331. <https://doi.org/10.1016/j.coi.2012.10.004> PMID: 23131610
6. Scheinecker C, Zwolfer B, Koller M, Manner G, Smolen JS. Alterations of dendritic cells in systemic lupus erythematosus: phenotypic and functional deficiencies. *Arthritis Rheum-U.S.* 2001; 44(4):856–65. Epub 2001/04/24. [https://doi.org/10.1002/1529-0131\(200104\)44:4<856::AID-ANR142>3.0.CO;2-A](https://doi.org/10.1002/1529-0131(200104)44:4<856::AID-ANR142>3.0.CO;2-A) PMID: 11315925.
7. Hoffman RW. T cells in the pathogenesis of systemic lupus erythematosus. *Clin Immunol*. 2004; 113(1):4–13. Epub 2004/09/24. <https://doi.org/10.1016/j.clim.2004.05.001> PMID: 15380523.
8. Bonelli M, von Dalwigk K, Savitskaya A, Smolen JS, Scheinecker C. Foxp3 expression in CD4+ T cells of patients with systemic lupus erythematosus: a comparative phenotypic analysis. *Ann Rheum Dis*. 2008; 67(5):664–71. Epub 2007/08/31. <https://doi.org/10.1136/ard.2007.074690> PMID: 17728327.
9. Hadaschik EN, Wei X, Leiss H, Heckmann B, Niederreiter B, Steiner G, et al. Regulatory T cell-deficient scurfy mice develop systemic autoimmune features resembling lupus-like disease. *Arthritis Res Ther*. 2015; 17:35. Epub 2015/04/19. PubMed Central PMCID: PMC4391674. <https://doi.org/10.1186/s13075-015-0538-0> PMID: 25890083
10. Ronnblom L, Eloranta ML, Alm GV. The type I interferon system in systemic lupus erythematosus. *Arthritis Rheum*. 2006; 54(2):408–20. Epub 2006/02/01. <https://doi.org/10.1002/art.21571> PMID: 16447217.
11. Nacionales DC, Kelly KM, Lee PY, Zhuang H, Li Y, Weinstein JS, et al. Type I interferon production by tertiary lymphoid tissue developing in response to 2,6,10,14-tetramethyl-pentadecane (pristane). *Am J Pathol*. 2006; 168(4):1227–40. PubMed Central PMCID: PMCPMC1606560. <https://doi.org/10.2353/ajpath.2006.050125> PMID: 16565497
12. Bennett L, Palucka AK, Arce E, Cantrell V, Borvak J, Banchereau J, et al. Interferon and granulopoiesis signatures in systemic lupus erythematosus blood. *J Exp Med*. 2003; 197(6):711–23. PubMed Central PMCID: PMCPMC2193846. <https://doi.org/10.1084/jem.20021553> PMID: 12642603
13. Kong KO, Tan AW, Thong BY, Lian TY, Cheng YK, Teh CL, et al. Enhanced expression of interferon-inducible protein-10 correlates with disease activity and clinical manifestations in systemic lupus erythematosus. *Clin Exp Immunol*. 2009; 156(1):134–40. PubMed Central PMCID: PMCPMC2673751. <https://doi.org/10.1111/j.1365-2249.2009.03880.x> PMID: 19175619
14. Ma X, Liu Q. MicroRNAs in the pathogenesis of systemic lupus erythematosus. *International journal of rheumatic diseases*. 2013; 16(2):115–21. Epub 2013/06/19. <https://doi.org/10.1111/1756-185X.12083> PMID: 23773633.
15. Perry D, Sang A, Yin Y, Zheng YY, Morel L. Murine models of systemic lupus erythematosus. *J Biomed Biotechnol*. 2011; 2011:271694. PubMed Central PMCID: PMCPMC3042628. <https://doi.org/10.1155/2011/271694> PMID: 21403825
16. Dai R, Zhang Y, Khan D, Heid B, Caudell D, Crasta O, et al. Identification of a common lupus disease-associated microRNA expression pattern in three different murine models of lupus. *PLoS One*. 2010; 5(12):e14302. Epub 2010/12/21. PubMed Central PMCID: PMC3000827. <https://doi.org/10.1371/journal.pone.0014302> PMID: 21170274
17. Xu Y, Zeumer L, Reeves WH, Morel L. Induced murine models of systemic lupus erythematosus. *Methods Mol Biol*. 2014; 1134:103–30. https://doi.org/10.1007/978-1-4939-0326-9_9 PMID: 24497358.
18. Reeves WH, Lee PY, Weinstein JS, Satoh M, Lu L. Induction of autoimmunity by pristane and other naturally occurring hydrocarbons. *Trends Immunol*. 2009; 30(9):455–64. Epub 2009/08/25. PubMed Central PMCID: PMC2746238. <https://doi.org/10.1016/j.it.2009.06.003> PMID: 19699150

19. Han S, Zhuang H, Xu Y, Lee P, Li Y, Wilson JC, et al. Maintenance of autoantibody production in pristane-induced murine lupus. *Arthritis Res Ther*. 2015; 17:384. PubMed Central PMCID: PMC4718029. <https://doi.org/10.1186/s13075-015-0886-9> PMID: 26717913
20. Dahlgren J, Takhar H, Anderson-Mahoney P, Kotlerman J, Tarr J, Warshaw R. Cluster of systemic lupus erythematosus (SLE) associated with an oil field waste site: a cross sectional study. *Environ Health*. 2007; 6:8. Epub 2007/02/24. PubMed Central PMCID: PMC1821321. <https://doi.org/10.1186/1476-069X-6-8> PMID: 17316448
21. Filipowicz W, Bhattacharyya SN, Sonenberg N. Mechanisms of post-transcriptional regulation by microRNAs: are the answers in sight? *Nat Rev Genet*. 2008; 9(2):102–14. Epub 2008/01/17. <https://doi.org/10.1038/nrg2290> PMID: 18197166.
22. Bluml S, Bonelli M, Niederreiter B, Puchner A, Mayr G, Hayer S, et al. Essential role of microRNA-155 in the pathogenesis of autoimmune arthritis in mice. *Arthritis Rheum-U.S.* 2011; 63(5):1281–8. Epub 2011/02/16. <https://doi.org/10.1002/art.30281> PMID: 21321928.
23. Leng RX, Pan HF, Qin WZ, Chen GM, Ye DQ. Role of microRNA-155 in autoimmunity. *Cytokine Growth Factor Rev*. 2011; 22(3):141–7. Epub 2011/06/28. <https://doi.org/10.1016/j.cytogfr.2011.05.002> PMID: 21703910.
24. Hu R, O'Connell RM. MicroRNA control in the development of systemic autoimmunity. *Arthritis research & therapy*. 2013; 15(1):202. Epub 2013/02/06. PubMed Central PMCID: PMC3672787. <https://doi.org/10.1186/ar4131> PMID: 23379780
25. O'Connell RM, Kahn D, Gibson WS, Round JL, Scholz RL, Chaudhuri AA, et al. MicroRNA-155 promotes autoimmune inflammation by enhancing inflammatory T cell development. *Immunity*. 2010; 33(4):607–19. Epub 2010/10/05. PubMed Central PMCID: PMC2966521. <https://doi.org/10.1016/j.immuni.2010.09.009> PMID: 20888269
26. Kohlhaas S, Garden OA, Scudamore C, Turner M, Okkenhaug K, Vigorito E. Cutting edge: the Foxp3 target miR-155 contributes to the development of regulatory T cells. *J Immunol*. 2009; 182(5):2578–82. <https://doi.org/10.4049/jimmunol.0803162> PMID: 19234151.
27. Thai TH, Patterson HC, Pham DH, Kis-Toth K, Kaminski DA, Tsokos GC. Deletion of microRNA-155 reduces autoantibody responses and alleviates lupus-like disease in the Fas(lpr) mouse. *Proc Natl Acad Sci U S A*. 2013; 110(50):20194–9. PubMed Central PMCID: PMC3864325. <https://doi.org/10.1073/pnas.1317632110> PMID: 24282294
28. Zhou S, Wang Y, Meng Y, Xiao C, Liu Z, Brohawn P, et al. In Vivo Therapeutic Success of MicroRNA-155 Antagomir in a Mouse Model of Lupus Alveolar Hemorrhage. *Arthritis Rheumatol*. 2016; 68(4):953–64. <https://doi.org/10.1002/art.39485> PMID: 26556607.
29. Xin Q, Li J, Dang J, Bian X, Shan S, Yuan J, et al. miR-155 Deficiency Ameliorates Autoimmune Inflammation of Systemic Lupus Erythematosus by Targeting S1pr1 in Fas(lpr) Mice. *J Immunol*. 2015; 194(11):5437–45. <https://doi.org/10.4049/jimmunol.1403028> PMID: 25911753.
30. Leiss H, Niederreiter B, Bandur T, Schwarzecker B, Bluml S, Steiner G, et al. Pristane-induced lupus as a model of human lupus arthritis: involvement of autoantibodies, internal organ and joint inflammation. *Lupus*. 2013; 22(8):778–92. Epub 2013/07/03. <https://doi.org/10.1177/0961203313492869> PMID: 23817510.
31. Leng RX, Pan HF, Qin WZ, Chen GM, Ye DQ. Role of microRNA-155 in autoimmunity. *Cytokine Growth Factor Rev*. 2011; 22(3):141–7. <https://doi.org/10.1016/j.cytogfr.2011.05.002> PMID: 21703910.
32. Jacob N, Yang H, Pricop L, Liu Y, Gao X, Zheng SG, et al. Accelerated pathological and clinical nephritis in systemic lupus erythematosus-prone New Zealand Mixed 2328 mice doubly deficient in TNF receptor 1 and TNF receptor 2 via a Th17-associated pathway. *J Immunol*. 2009; 182(4):2532–41. Epub 2009/02/10. PubMed Central PMCID: PMC2790862. <https://doi.org/10.4049/jimmunol.0802948> PMID: 19201910
33. Weening JJ, D'Agati VD, Schwartz MM, Seshan SV, Alpers CE, Appel GB, et al. The classification of glomerulonephritis in systemic lupus erythematosus revisited. *J Am Soc Nephrol*. 2004; 15(2):241–50. Epub 2004/01/30. PMID: 14747370.
34. Parfitt AM, Drezner MK, Glorieux FH, Kanis JA, Malluche H, Meunier PJ, et al. Bone histomorphometry: standardization of nomenclature, symbols, and units. Report of the ASBMR Histomorphometry Nomenclature Committee. *J Bone Miner Res*. 1987; 2(6):595–610. Epub 1987/12/01. <https://doi.org/10.1002/jbmr.5650020617> PMID: 3455637.
35. Redlich K, Gortz B, Hayer S, Zwerina J, Doerr N, Kostenuik P, et al. Repair of local bone erosions and reversal of systemic bone loss upon therapy with anti-tumor necrosis factor in combination with osteoprotegerin or parathyroid hormone in tumor necrosis factor-mediated arthritis. *The American journal of pathology*. 2004; 164(2):543–55. Epub 2004/01/27. PubMed Central PMCID: PMC1602264. [https://doi.org/10.1016/S0002-9440\(10\)63144-6](https://doi.org/10.1016/S0002-9440(10)63144-6) PMID: 14742260

36. McKenzie WN Jr., Sunderrajan EV, Kavanaugh JL, Braun S, Ansbacher L, Walker SE. Sex hormones modulate the response of pulmonary perivascular inflammation to cyclophosphamide therapy in MRL/MpJ-lpr/lpr mice. *Am J Pathol*. 1988; 131(3):530–8. Epub 1988/06/01. PMID: [3381881](#); PubMed Central PMCID: PMC1880696.
37. Schett G, Tuerk B. Bone histomorphometry in arthritis models. *Methods in molecular medicine*. 2007; 135:269–83. Epub 2007/10/24. PMID: [17951665](#).
38. Eferl R, Hasselblatt P, Rath M, Popper H, Zenz R, Komnenovic V, et al. Development of pulmonary fibrosis through a pathway involving the transcription factor Fra-2/AP-1. *Proceedings of the National Academy of Sciences of the United States of America*. 2008; 105(30):10525–30. Epub 2008/07/22. PubMed Central PMCID: PMC2492511. <https://doi.org/10.1073/pnas.0801414105> PMID: [18641127](#)
39. Leonard JP, Lacasce AS, Smith MR, Noy A, Chirieac LR, Rodig SJ, et al. Selective CDK4/6 inhibition with tumor responses by PD0332991 in patients with mantle cell lymphoma. *Blood*. 2012. Epub 2012/03/03. <https://doi.org/10.1182/blood-2011-10-388298> PMID: [22383795](#).
40. Uderhardt S, Herrmann M, Oskolkova OV, Aschermann S, Bicker W, Ipseiz N, et al. 12/15-lipoxygenase orchestrates the clearance of apoptotic cells and maintains immunologic tolerance. *Immunity*. 2012; 36(5):834–46. Epub 2012/04/17. <https://doi.org/10.1016/j.immuni.2012.03.010> PMID: [22503541](#).
41. Stummvoll GH, DiPaolo RJ, Huter EN, Davidson TS, Glass D, Ward JM, et al. Th1, Th2, and Th17 effector T cell-induced autoimmune gastritis differs in pathological pattern and in susceptibility to suppression by regulatory T cells. *Journal of immunology*. 2008; 181(3):1908–16. Epub 2008/07/22. PMID: [18641328](#); PubMed Central PMCID: PMC2561289.
42. Chowdhary VR, Grande JP, Luthra HS, David CS. Characterization of haemorrhagic pulmonary capillaritis: another manifestation of Pristane-induced lupus. *Rheumatology (Oxford)*. 2007; 46(9):1405–10. Epub 2007/06/20. <https://doi.org/10.1093/rheumatology/kem117> PMID: [17576695](#).
43. Huffaker TB, Hu R, Runtsch MC, Bake E, Chen X, Zhao J, et al. Epistasis between microRNAs 155 and 146a during T cell-mediated antitumor immunity. *Cell Rep*. 2012; 2(6):1697–709. PubMed Central PMCID: PMC3628775. <https://doi.org/10.1016/j.celrep.2012.10.025> PMID: [23200854](#)
44. Rodriguez A, Vigorito E, Clare S, Warren MV, Couttet P, Soond DR, et al. Requirement of bic/microRNA-155 for normal immune function. *Science*. 2007; 316(5824):608–11. Epub 2007/04/28. PubMed Central PMCID: PMC2610435. <https://doi.org/10.1126/science.1139253> PMID: [17463290](#)
45. Lu LF, Thai TH, Calado DP, Chaudhry A, Kubo M, Tanaka K, et al. Foxp3-dependent microRNA155 confers competitive fitness to regulatory T cells by targeting SOCS1 protein. *Immunity*. 2009; 30(1):80–91. PubMed Central PMCID: PMC2654249. <https://doi.org/10.1016/j.immuni.2008.11.010> PMID: [19144316](#)
46. Gracias DT, Stelekati E, Hope JL, Boesteanu AC, Doering TA, Norton J, et al. The microRNA miR-155 controls CD8(+) T cell responses by regulating interferon signaling. *Nat Immunol*. 2013; 14(6):593–602. PubMed Central PMCID: PMC3664306. <https://doi.org/10.1038/ni.2576> PMID: [23603793](#)
47. O'Connell RM, Taganov KD, Boldin MP, Cheng G, Baltimore D. MicroRNA-155 is induced during the macrophage inflammatory response. *Proc Natl Acad Sci U S A*. 2007; 104(5):1604–9. PubMed Central PMCID: PMC1780072. <https://doi.org/10.1073/pnas.0610731104> PMID: [17242365](#)